Dalton Transactions

Heptamolybdate: A Highly Active Sulfide Oxygenation Catalyst

Journal:	*Dalton Transactions*
Manuscript ID	DT-ART-02-2018-000583.R2
Article Type:	Paper
Date Submitted by the Author:	21-May-2018

Complete List of Authors:	Porter, Ashlin ; Purdue University Hu, Hanfeng; Purdue University Liu, Xuemei; Xi'an Shiyou University, Raghavan, Adharsh ; Purdue University Adhikari, Sarju; Purdue University College of Health and Human Sciences Hall, Derrick ; Purdue University Thompson, Dylan ; Purdue University Liu, Bin; Purdue University Xia, Yu; Purdue University, Ren, Tong; Purdue University,

Dalton Transactions

ARTICLE

Heptamolybdate: A Highly Active Sulfide Oxygenation Catalyst

Ashlin G. Porter,[a] Hanfeng Hu,[a] Xuemei Liu,[b] Adharsh Raghavan,[a] Sarju Adhikari,[a] Derrick R. Hall,[a] Dylan J. Thompson,[a] Bin Liu,[a] Yu Xia*[a] and Tong Ren*[a]

Received 00th January 20xx,
Accepted 00th January 20xx

DOI: 10.1039/x0xx00000x

www.rsc.org/

The sulfide oxygenation activities of both heptamolybdate ($[Mo_7O_{24}]^{6-}$, $[\mathbf{1}]^{6-}$) and its peroxo adduct $[Mo_7O_{22}(O_2)_2]^{6-}$ ($[\mathbf{2}]^{6-}$) were examined in this contribution. $[Mo_7O_{22}(O_2)_2]^{6-}$ was prepared in a yield of 65% from $(NH_4)_6[Mo_7O_{24}]$ (**1a**) upon treatment of 10 equiv of H_2O_2 and structurally identified through single crystal X-ray diffraction study. $(n\text{Bu}_4\text{N})_6[Mo_7O_{22}(O_2)_2]$ (**2b**) is an efficient catalyst for the sequential oxygenation of methyl phenyl sulfide (MPS) by H_2O_2 to the corresponding sulfoxide and subsequently sulfone with a 100% utility of H_2O_2. Surprisingly, $(n\text{Bu}_4\text{N})_6[Mo_7O_{24}]$ (**1b**) is a significantly faster catalyst than **2b** for MPS oxygenation under identical conditions. The pseudo-first order k_{cat} constants from initial rate kinetics are 54 $M^{-1}s^{-1}$ and 19 $M^{-1}s^{-1}$ for **1b** and **2b**, respectively. Electrospray ionization mass spectrometry (ESI-MS) investigation of **1b** under the catalytic reaction conditions revealed that $[Mo_2O_{11}]^{2-}$ is likely the main active species in sulfide oxygenation by H_2O_2.

Introduction

The oxygenation of organic sulfides is a transformation key to medicinal chemistry,[1] petroleum desulfurization,[2] and nerve agent detoxification.[3-5] Highly relevant to the latter two applications are both the reaction rates and the use of inexpensive oxidants and catalysts. Hydrogen peroxide and *tert*-butyl hydroperoxide (TBHP) are among the desired oxidants because of their low costs and environmentally friendly nature.[6] Hydrogen peroxide is the most studied oxidant, and can be activated with a variety of transition metal based homogeneous catalysts. Among a plethora of catalysts reported,[7] homo- and hetero-polyoxometalates (POMs) stand out due to both the ease of preparation and their chemical robustness.[8-10] Recent examples of sulfide oxygenation catalyzed by both POMs and related species include the degradation of mustard agent simulants,[11-13] oxygenation of thioanisole with $(Bmim)_2[Mo_6O_{19}]$ (Bmim = 1-butyl-3-methylimidazolium),[14] conversion of 2-chloroethyl ethyl sulfide to its sulfoxide using $H_3PW_{12}O_{40}$ embedded in a MOF,[15] and the selective formation of sulfoxide as the precursor of vinyl glycine.[16] Contributions from our laboratory include the early demonstration of excellent chemical selectivity and efficient use of H_2O_2 in sulfide oxygenation using $[\gamma\text{-}SiW_{10}O_{34}(H_2O)_2]^{4-}$,[17] its subsequent heterogenization in amine functionalized MCM-41,[18] and the recent discovery of peroxo-dimolybdate as a highly efficient catalyst.[19]

Heptamolybdate, $[Mo_7O_{24}]^{6-}$ (also known as paramolybdate), is the lowest member of the isopolymolybdate family,[20] and its ammonium salt ($(NH_4)_6[Mo_7O_{24}]$, **1a**) is commercially available and inexpensive. While heteropolyoxometallates have attracted intense interest as oxygenation catalysts,[9, 10] the role of heptamolybdate as an oxygenation catalyst has been sparingly explored. Noteworthy among a handful of examples using $[Mo_7O_{24}]^{6-}$ as a catalyst are the olefin epoxidation and alcohol oxidation by H_2O_2[21] and the conversion of dibenzothiophene and derivatives to corresponding sulfones by H_2O_2 in ionic liquid.[22] Also noteworthy is the ability of heptamolybdate to promote hydrolysis of phosphoesters.[23] Reported herein are the preparation and structural characterization of a di-peroxo derivative of heptamolybdate, $[Mo_7O_{22}(O_2)_2]^{6-}$ ($[\mathbf{2}]^{6-}$), and its activity in promoting sulfide oxygenation by H_2O_2. It was discovered in the process of performing control experiments that the parent heptamolybdate is a far more active catalyst. The reactivity scope, catalytic rates and the nature of the active species under the catalytic conditions were carefully examined.

Results and discussion

Synthesis and structural identification of $[Mo_7O_{22}(O_2)_2]^{6-}$ ($[\mathbf{2}]^{6-}$)

Curious about the nature of the active species in the aforementioned olefin epoxidation and alcohol oxidation reactions catalyzed by heptamolybdate,[21, 24] we first sought to identify the predominant species produced upon treatment of $[Mo_7O_{24}]^{6-}$ with H_2O_2. Hence, an aqueous solution of $(NH_4)_6[Mo_7O_{24}]$ (**1a**) was treated with 10 equiv of H_2O_2 in the presence of 2.5 equiv guanidinium ($CH_6N_3^+$) chloride, and $(NH_4)_4(CH_6N_3)_2[Mo_7O_{22}(O_2)_2]$ (**2a**) was isolated as yellow crystalline materials in a yield of 65% upon slow evaporation of the reaction mixture. X-ray diffraction study verified the above-mentioned formula of **2a** with lattice water molecules. Compared to the parent ion $[Mo_7O_{24}]^{6-}$, one of the terminal oxos on both the Mo3 and Mo5 centers were replaced by a peroxo group in forming the di-peroxo heptamolybdate anion $[Mo_7O_{22}(O_2)_2]^{6-}$, as shown in Figure 1. Both of the peroxo-bound molybdenum centers (Mo3 and Mo5) are seven-coordinated. The pentagonal bipyramidal arrangement of coordination is frequently observed in peroxo complexes. The bond lengths of the peroxo moiety in **2a** are 1.44(2) and 1.34(2) Å, respectively, falling in the expected range for Mo/W peroxo compounds.[25]

[a] Department of Chemistry, Purdue University, 560 Oval Drive, West Lafayette, IN 47906, USA.yxia@purdue.edu; tren@purdue.edu
[b] College of Chemistry and Chemical Engineering, Xi'an Shiyou University, Xi'an, China

† Dedicated to Professor Kim Dunbar on the occasion of her 60th Birthday.
Electronic Supplementary Information (ESI) available: [details of any supplementary information available should be included here]. See DOI: 10.1039/x0xx00000x

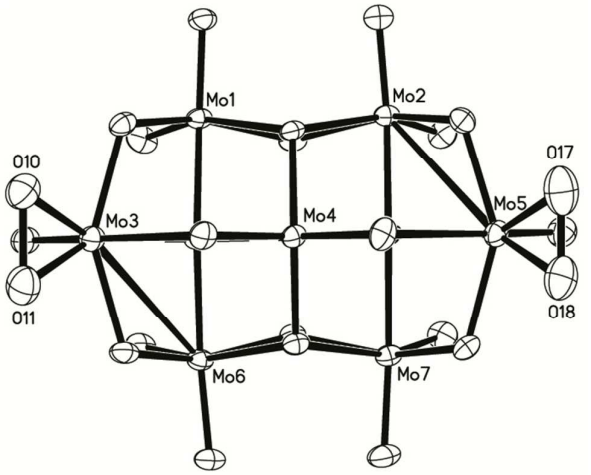

Fig. 1 Structural plot of $[Mo_7O_{22}(O_2)_2]^{6-}$ in **2a**. Counter ions and lattice water molecules were omitted for clarity; the CIF has been deposited with the Cambridge Crystallographic Data Centre (CCDC 1839304).

Sulfide oxygenation activity of $[Mo_7O_{22}(O_2)_2]^{6-}$ and $[Mo_7O_{24}]^{6-}$

Upon the structural identification of the di-peroxo species $[\mathbf{2}]^{6-}$, its activity in facilitating H_2O_2 oxygenation was examined with methyl phenyl sulfide (MPS, also known as thioanisole) as the substrate. With **2b** ($(Bu_4N)_6[Mo_7O_{22}(O_2)_2]$) at 1 mol% loading and the use of two equiv of H_2O_2, MPS was completely consumed in 10 min as indicated by GC analysis (Table 1), demonstrating the efficacy of $[\mathbf{2}]^{6-}$ in promoting H_2O_2 oxygenation. Furthermore, full conversion of MPS to sulfone ($MPSO_2$) was accomplished in 5h in the same reaction, indicating a 100% utility of active oxygen in H_2O_2. Previously, our laboratory reported that a divacant lacunary silicotungstate, $[\gamma\text{-}SiW_{10}O_{34}(H_2O)_2]^{4-}$, catalyzes H_2O_2 oxygenation of organic sulfides with a 100% utility of H_2O_2.[17] However, the catalytic reaction with divacant silicotungstate is significantly slower than those with **2b** even in the presence of the best co-catalyst, and the preparation of divacant silicotungstate is laborious. Clearly, **2b** is a simple and yet much more efficient catalyst for H_2O_2 oxygenation.

Encouraged by the performance of **2b**, the activity of heptamolybdate was examined in a control experiment. Similar to the conditions used with **2b**, MPS was treated with two equiv of H_2O_2 in the presence of 1 mol% $(Bu_4N)_6[Mo_7O_{24}]$ (**1b**). Surprisingly, **1b** is significantly faster than **2b**, consuming almost all MPS in 2 min with 100% consumption achieved in under 5 min (Table 1). It is clear from Table 1 that **1b** is also significantly faster than **2b** in converting sulfoxide (MPSO) to sulfone ($MPSO_2$).

Table 1. Sulfide oxidation of MPS catalysed by **1b** and **2b**.

Time (min)	Catalyst	MPS (%)	MPSO (%)	$MPSO_2$ (%)
2	1b	1	71	28
	2b	37	60	3
5	1b	0	46	54
	2b	4	81	14
8	1b	0	40	59
	2b	1	79	20
10	1b	0	38	62
	2b	0	69	30
15	1b	0	29	71
	2b	0	56	44
30	1b	0	12	88
	2b	0	34	66
60	1b	0	2	98
	2b	0	16	84
120	1b	0	1	99
	2b	0	2	98
180	1b	0	1	99
	2b	0	1	99
240	1b	0	0	100
	2b	0	1	99
300	1b	0	0	100
	2b	0	0	100

[a] Each reaction was carried out with 0.50 mmol MPS, 1.0 mmol H_2O_2, and 0.0050 mmol **1b/2b** (1 mol% loading) in 5 mL CH_3CN at room temperature.

The fast oxygenation facilitated by **1b** also prompted further exploration into whether the oxygenation occurs in a stepwise fashion. The reaction was conducted at a reduced level of catalyst loading (0.2 mol% with respect to MPS), and the distribution of products was monitored with GC. The resultant speciation curves are shown in Figure 2, which indicates the presence of $MPSO_2$ (*ca.* 20%) at the time of full consumption of MPS around 10 min. Clearly, the oxygenation catalyzed by **1b** is not step-wise. It is also apparent from Figure 2 that there is no observable induction period.

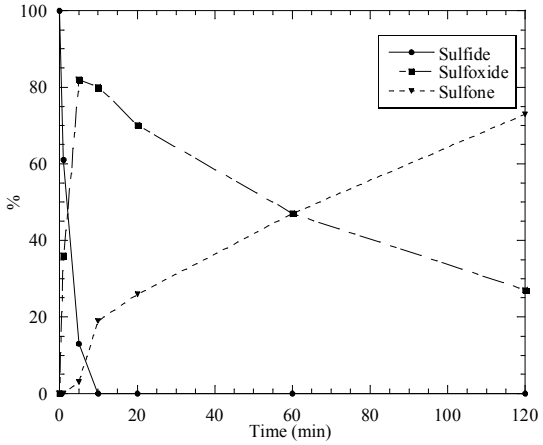

Fig. 2 Speciation curve of H_2O_2-oxygenation of MPS catalyzed by **1b** conducted with 0.50 mmol MPS, 1.0 mmol H_2O_2 and 0.0010 mmol **1b** in 5 mL CH_3CN at room temperature.

Catalytic oxygenation of other organic sulfides with $[Mo_7O_{24}]^{6-}$

Oxygenation of organic sulfides is relevant to current technologies such as the preparation of chiral sulfoxides in medicinal chemistry,[26]

chemical degradation of *V*-type nerve agents,[27] and deep desulfurization of fossil fuels.[2] Hence, the proficiency of **1** in facilitating deep oxygenation was tested using a variety of sulfide substrates including DBT (dibenzothiophene), and results are collected in Table 2. All entries in Table 2 are equal in catalyst loading (0.1 mol%) and use of two equiv of H_2O_2 except DBT. It is clear from Table 2 that the fastest conversions to sulfone were accomplished within one hour for PTE (phenyl thioethanol) and BPS (benzyl phenyl sulfide), which are the most electron-rich among the substrates listed. Electron poor 4BT (4-bromothioanisole) and PPS (phenylsulfide) required longer reaction times to fully convert. Plausibly, the faster electrophilic oxygenation of the more electron rich sulfides resulted in a faster formation of sulfone. Being the most sterically hindered substrate DBT required a much longer conversion time and H_2O_2 in 100% excess. DBT and its methyl derivatives, known as refractory sulphides, are the primary targets of fuel desulfurization,[2] and **1** could be a relevant catalyst. In addition, oxygenation of sulphides catalyzed by **2b** were carried out under the same conditions as those for reactions with **1b** and the times required for complete conversion to the corresponding sulphone (Table 2) are much longer than those with **1b**, consistent with the result of MPS oxygenation.

Table 2. Oxygenation of additional sulfides with **1b** and **2b** [a]

Sulfide	Abbreviation	H_2O_2 equiv	**1b** *t*/hr [b]	**2b** *t*/hr [b]
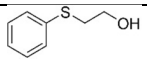	PTE	2	1	2
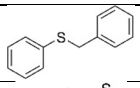	BPS	2	1	3
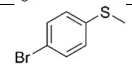	4BT	2	2	4
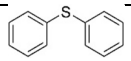	PPS	2	3.5	7
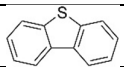	DBT[c]	4	9	36

[a] The reaction was carried out with 0.5 mmol sulfide, 1.0 mmol H_2O_2 and 0.1 mol% **1b** / **2b** in 5 mL MeCN at 22 °C

[b] Time for complete conversion to sulfo ne.

[c] 4 equiv of H_2O_2 was used for the DBT reaction

Initial rate kinetics

Given the extraordinary efficiency of both $[\mathbf{1}]^{6-}$ and $[\mathbf{2}]^{6-}$ in promoting sulfide oxygenation and a potentially complex reaction mechanism due to their multinuclear nature, the reaction rate dependence on catalyst concentration was investigated based on the initial rate method. While both MPS (1.21 mM) and H_2O_2 (23 mM) were present in large excess in order to maintain pseudo first order conditions, the concentration of **1b** was varied from 0.003 mM to 0.036 mM (0.25 to 3.0 mol% loading with respect to MPS), and that of **2b** from 0.024 mM to 0.12 mM (2.0 to 10 mol% with respect to MPS). Monitoring the disappearance of MPS at 290 nm, the k_{obs} at a specific catalyst concentration was determined by fitting the first 15 min trace using a first order equation (ln(*Abs*) versus *t*), and the resultant k_{obs} vs. [cat] plots are shown in Figure 3 for both **1b** and **2b**. It is clear from Figure 3 that fitting both k_{obs} vs. [cat] data sets yielded excellent linear correlations, and the slopes yielded k_{cat} values of 54 $M^{-1}sec^{-1}$ and 19 $M^{-1}sec^{-1}$ for **1b** and **2b**, respectively. Consistent with the data presented in Table 1, k_{cat}(**1b**) is significantly larger than k_{cat}(**2b**). Previously, k_{cat} for the same H_2O_2 oxygenation of MPS was reported to be about 11 $M^{-1}min^{-1}$ for $[\{MoO(O_2)_2\}_2(\mu\text{-}O)]^{2-}$ by our laboratory[19] and 9.3 $M^{-1}sec^{-1}$ for $[SeO_4\{\mu\text{-}WO(O_2)_2\}_2]^{2-}$ by Kamata *et al.*,[28] which were among the fastest oxygenation catalysts based on molybdates/tungstates. Clearly, heptamolybdate offers the advantage of being a superior catalyst without the requirement of elaborate synthesis.

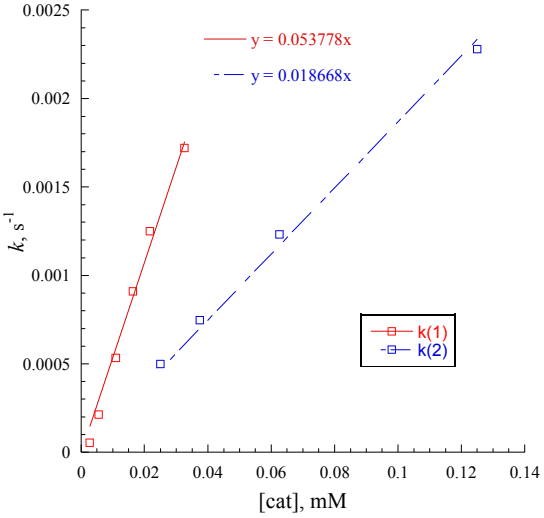

Fig. 3 Rate dependence on the concentrations of **1b** (red) and **2b** (blue) under pseudo-first order conditions.

The significant contrast in k_{cat} between $[\mathbf{1}]^{6-}$ and $[\mathbf{2}]^{6-}$ may signal a difference in the active catalytic species. To gain an insight into the nature of possible active species, UV-vis spectra of **1b** and **2b** as pure compounds and in the presence of H_2O_2 in large excess were examined, and the results are shown in Figure 4. Compound **1b** (blue solid, **A**) has a broad peak with a λ_{max} of 220 nm, while compound **2b** displays a sharper peak with a λ_{max} of 252 nm (red solid, **C**). Upon the addition of H_2O_2 (232 equiv) to **1b** and a five min incubation time, the broad peak at 220 nm disappeared and a weaker, broader peak appeared at a λ_{max} of 330 nm (blue dash, **B**). Interestingly, the addition of H_2O_2 (232 equiv) to **2b** only led to a slight intensification of the 252 nm peak, but no new features. Clearly, while both **1b** and **2b** catalyze oxygenation reactions efficiently, the active species generated in the presence of excess H_2O_2 are different. More importantly, the treatment of **1b** with excess H_2O_2 does *not* result in **2b** *in acetonitrile*.

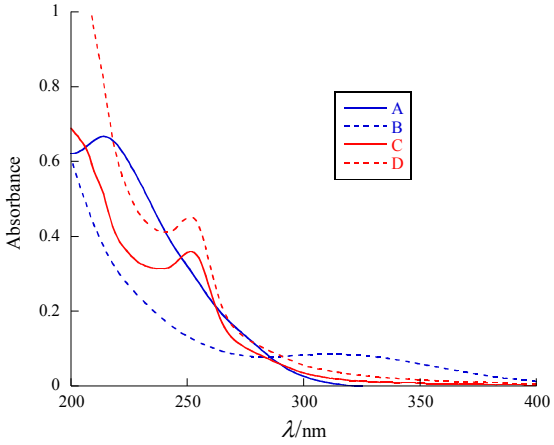

Fig. 4 Absorption spectra in acetonitrile of **1b** before (**A**, 1.75 mM) and after the addition of 232 equiv of H_2O_2 (**B**); **2b** before (**C**, 3.27 mM) and after the addition of 232 equiv of H_2O_2 (**D**).

Identification of intermediates though mass spectrometry

It became clear from both the kinetics and UV-vis studies that the active intermediate is not the same for **1b** and **2b**. Hence, the *in situ* nano-electrospray ionization mass spectrometric (nanoESI-MS) technique[29, 30] was utilized to identify the active intermediate(s) for both [**1**]$^{6-}$ and [**2**]$^{6-}$ under three sets of experimental conditions: (**I**) **1b** and **2b** alone in acetonitrile; (**II**) **1b** and **2b** with H_2O_2 in large excess in acetonitrile and (**III**) **1b** and **2b** with MPS and H_2O_2 in large excess, i.e. the conditions of a typical catalytic reaction.

The negative mode ESI-MS spectrum of neat **1b** in acetonitrile (Fig. S1 in the supplementary information) features major ion fragments $[Mo_4O_{13}]^{2-}$ (*m/z* 295.9), $[Mo_3O_{10}]^{2-}$ (*m/z* 225.0) and $[Mo_5O_{16}]^{2-}$ (*m/z* 368.4), while the parent ion $[Mo_7O_{24}]^{6-}$ (*m/z* 175.9) was not detected. Previously, Walanda *et al.* studied the aqueous solution of isopolyoxomolybdates using ESI-MS and reported the omnipresence of the $[Mo_mO_{3m+1}]^{2-}$ type ions and the detection of parent ion $[Mo_7O_{24}]^{6-}$ at pH = 6.[31] Our detection of $[Mo_3O_{10}]^{2-}$, $[Mo_4O_{13}]^{2-}$ and $[Mo_5O_{16}]^{2-}$ despite the difference in solvent conditions indicates a similar fragmentation pattern of $[Mo_7O_{24}]^{6-}$ in acetonitrile. The absence of the parent ion peak likely reflects the fragility of $[Mo_7O_{24}]^{6-}$ in a non-aqueous media. The negative mode ESI-MS spectrum of neat **2b** (Fig. S2 in the supplementary information) contains a noteworthy fragment corresponding to $[Mo_2O_{11}]^{2-}$ (*m/z* 183.8), and it does not display any of the significant ion fragment peaks identified for **1b**.

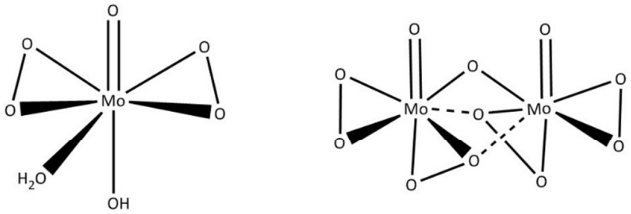

$[H_3MoO_7]^-$ $[Mo_2O_{11}]^{2-}$

Scheme 1. Peroxy-intermediate derived from $[Mo_7O_{24}]^{6-}$

The negative mode ESI-MS spectrum of **1b** in the presence of 100-fold H_2O_2 was acquired to gain insight into the interaction between H_2O_2 and isopolymolybdate species, as well as the likely resultant species. Strikingly but unsurprisingly, most of the aforementioned $[Mo_mO_{3m+1}]^{2-}$ type ions vanished with $[Mo_4O_{13}]^{2-}$ remaining as the only observable member. The spectrum (Fig. 5a) features three main ions at *m/z* values of 183.8, 191.8 and 210.8, which correlate respectively to the $[Mo_2O_{11}]^{2-}$, $[HMoO_6]^-$ and $[H_3MoO_7]^-$. Interestingly, the $[Mo_2O_{11}]^{2-}$ ion (see Scheme 1) was previously prepared and characterized as an active catalyst for H_2O_2 oxygenation by our laboratory.[19] The appearance of both $[H_3MoO_7]^-$ (Scheme 1) and $[HMoO_6]^-$ is also noteworthy, as the former is a member of the Mimoun species, i.e. $M(=O)(\eta^2\text{-}O_2)_2(H_2O)_2$ (M = Cr, Mo and W),[32, 33] and the latter is its dehydrated form. As shown in Fig. S3, collision-induced dissociation (CID) of the ion at *m/z* 210.8 ($[H_3MoO_7]^-$) produced a loss of water (-18 Da), further corroborating the aforementioned assignments of $[HMoO_6]^-$ and $[H_3MoO_7]^-$. It is noteworthy that the $[Mo_2O_{11}]^{2-}$ peak also appeared in the ESI-MS spectrum of **2b** in the presence of H_2O_2 (Fig. S4), but in significantly reduced abundance (BPI = 32.7%). The *in situ* ESI-MS technique was finally extended to the catalytic oxygenation of MPS, namely a solution containing MPS and H_2O_2 in 1:1 mole ratio and 1mol% of **1b**. Similar to the spectrum obtained in **II**, the predominant species observed are $[HMo_2O_{11}]^-$, $[HMoO_6]^-$ and $[H_3MoO_7]^-$ with respective BPIs of 49.4%, 31.7% and 19.4% shown in Figure 5b. Interestingly, the most abundant species (BPI = 100%) from experiment **III** is $[Mo_4O_{13}]^{2-}$ (*m/z* 295.9), which is also present in spectrum **II** but at a much lower abundance (BPI = 16.7%, see Fig. 5a). For comparison purpose, ESI-MS spectrum of **2b** under catalytic conditions was also taken (Fig. S5), which reveals the presence of $[H_3MoO_7]^-$ and $[HMo_2O_{11}]^-$ similar to the case of **1b** at relatively low BPI percentages of 6.99 and 20.06%, respectively. This result indicated that the lower activity of **2b** is likely due to the insufficient production of $[Mo_2O_{11}]^{2-}$ ion.

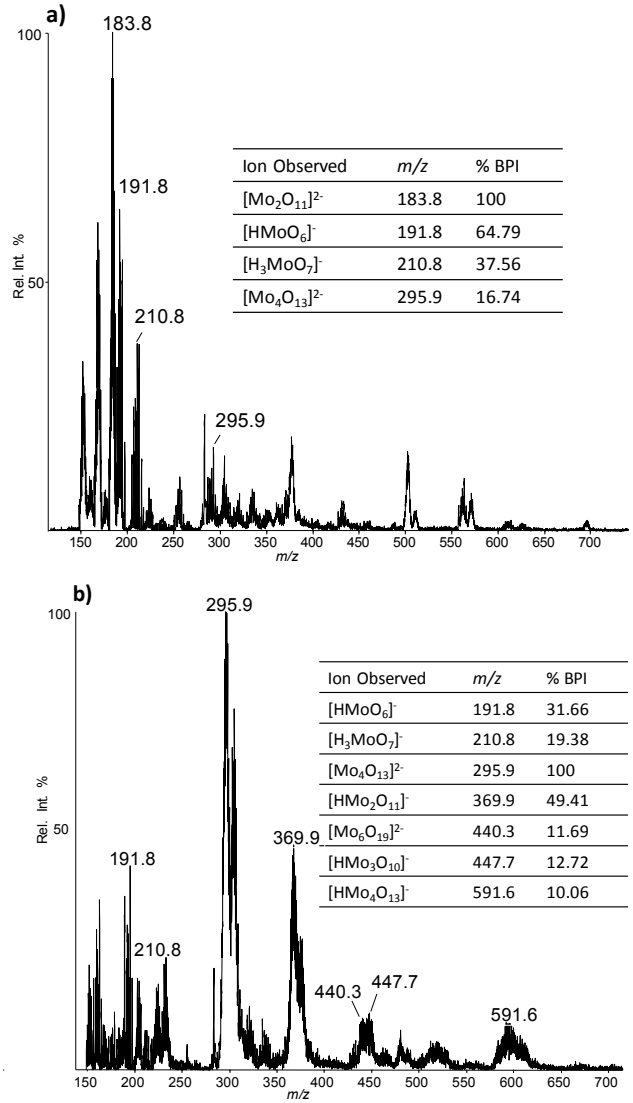

Fig. 5 NanoESI mass spectra of **1b** (a) 1 min after the addition of H_2O_2; (b) 1 min after the addition of both H_2O_2 of MPS.

Experimental

Materials and instrumentation

Acetonitrile, ammonium heptamolybdate tetrahydrate and guanidine hydrochloride were purchased from Sigma Aldrich. Tetra-*n*-butylammonium bromide was purchased from Alfa Aesar. Methyl phenyl sulfide, phenyl sulfide, benzyl phenyl sulfide, 4-bromothioanisole, phenylthioethanol and dibenzothiophene were

purchased from ACROS Organics. Hydrogen peroxide (30%) was purchased from Macron Fine Chemicals and standardized via iodometric titration. Oxygenation reaction samples were analyzed using an Agilent 7890A GC system equipped with a flame ionization detector. The separation of substrate and products was achieved using an Agilent HP-5 column with dimensions of 30 m x 0.320 mm with 25 micron film thickness. Reaction progress was monitored at 290 nm via UV-Vis spectroscopy on a JASCO V-670 Spectrophotometer.

Synthesis of $(n\text{-}Bu_4N)_6[Mo_7O_{24}]$ (1b)

Ammonium heptamolybdate tetrahydrate (500 mg, 0.405 mmol) was dissolved in water (4 mL). In a separate round bottom flask tetrabutylammonium bromide (0.789 g, 2.43 mmol) was dissolved in water (4 mL). The two solutions were mixed together and stirred for 10 minutes, with a white precipitate forming immediately. The precipitate was allowed to settle in the vial and collected by filtration and dried. Yield: 81% based on Mo.

Synthesis of $(n\text{-}Bu_4N)_6[Mo_7O_{22}(O_2)_2]\cdot nH_2O$ (2b)

Ammonium heptamolybdate tetrahydrate (2.472 g; 2.0 mmol) was dissolved in 20 mL water, to which were slowly added with stirring 2.0 mL 30% hydrogen peroxide (20 mmol) and tetrabutylammonium bromide (4.832 g, 15 mmol) in 10 mL water. After 30 min, the yellow precipitate was collected by filtering through a sintered glass filter, washed with 20 mL water, and air dried to afford powder samples 3.98 g of 2b (yield 78% based on Mo). Elemental analysis calcd (%) for $C_{96}H_{216}N_6Mo_7O_{26}$: C, 45.4; H, 8.6; N, 3.3; Mo, 26.4. Found (%):C, 43.8; H, 9.0; N, 3.1; Mo, 25.6. IR for 1 (KBr, cm^{-1}): 3394 (s), 2964 (m), 2940 (m), 2874 (m), 1647 (m), 1483 (m), 1460 (m), 1381 (m), 1348 (w), 1281 (w), 1152 (w), 1158 (w), 1069 (w),1030 (w), 1004 (w), 949 (m), 922 (s), 903 (s), 852 (s), 797 (vs), 730 (s), 657 (vs), 583 (s), 556 (s).

Catalytic conversion of sulfide

The catalyst (**1b**/**2b**) (0.005 mmol, 1 mol%) was dissolved in 5 mL of acetonitrile. Substrate sulfide (0.5 mmol) and internal standard 1,2-dichlorobenzene (0.4 mmol) were added to the reaction solution. H_2O_2 (1 mmol) was added to the solution drop wise, and the solution turned yellow. In the case of DBT additional equivalents of H_2O_2 (2 mmol total) were added in order to achieve complete conversion. Aliquots were taken at different time periods, quenched using MnO_2, and analyzed using GC.

Initial rate kinetics of 1b and 2b

Standard acetonitrile solutions utilized were prepared for **1b** at 1.75 mM, **2b** at 3.27 mM, MPS at 39 mM, and hydrogen peroxide at 0.37 M. Solutions for kinetic studies were prepared combining 200 µL of MPS and a specific volume of **1b** in a quartz cuvette, the volume of which was adjusted to 3.22 mL with additional acetonitrile. The reaction was initiated by the addition of 200 µL of the H_2O_2 stock solution. The absorbance of the solution at 290 nm was measured every 20 seconds for 30 minutes. The initial *in situ* concentrations upon the addition of H_2O_2 to the cuvette are 2.43 mM for MPS, 23 mM for H_2O_2, with a range of concentrations for **1b** (0.027-0.0326 mM) or **2b** (0.025-0.125 mM).

Nano-electrospray ionization mass spectra of 1b and 2b

For a typical measurement, a 5 mL solution of **1b** or **2b** (0.005 mmol in acetonitrile), 59 µL of MPS (0.5 mmol in acetonitrile) and 51 µL of H_2O_2 (0.5 mmol in acetonitrile) were combined. These same concentrations and volumes were used for the neat **1b/2b** (Experiment **I**) and **1b/2b** plus H_2O_2 (Experiment **II**) spectra collected**.** An aliquot (5 µL) was removed and promptly diluted in 1 mL acetonitrile, then sprayed using a home-built nano-ESI source.[29] All ESI-MS experiments for **1b** were performed in the negative ion mode on a 4000 QTRAP triplequadrupole/linear ion trap mass spectrometer (Sciex, Toronto, Canada). The characteristic parameters of the MS during this study were set as follows: spray voltage, 1500 V; curtain gas, 5 psi; declustering potential (DP), 20 V. Mass analysis was achieved by using Q3 as a linear ion trap at a scan rate of 1000 Da/s. Data shown here were typically averages of 50 scans. ESI-MS experimental conditions for **2b** are provided in the supplementary information. Data acquisition, processing, and instrument control were performed using Analyst 1.6 software.

Conclusions

It has been shown in this contribution that commodity chemical heptamolybdate is a highly efficient catalyst for hydrogen peroxide oxygenation of organic sulfides in terms of both the reaction rate and the hydrogen peroxide utility (100%). Electrospray ionization mass spectrometry studies revealed that the heptamolybdate ion undergoes significant fragmentation under the catalytic reaction conditions. One of the major ions detected in ESI-MS, $[Mo_2O_{11}]^{2-}$, has been identified as the main active species based on the consideration of catalytic rates. Our success herein will hopefully encourage further applications of ESI-MS and other MS techniques[35, 36] in polyoxometallate catalysis.

Conflicts of interest

There are no conflicts to declare.

Acknowledgements

We thank the financial support from Purdue University. Y. X. and H. H. acknowledge the support from NSF CHE-1308114.

Notes and references

1 I. Fernandez and N. Khair, *Chem. Rev.*, 2003, **103**, 3651.
2 I. V. Babich and J. A. Moulijn, *Fuel*, 2003, **82**, 607-631.
3 Y.-C. Yang, *Acc. Chem. Res.*, 1999, **32**, 109-115.
4 G. W. Wagner and Y. C. Yang, *Ind. Eng. Chem. Res.*, 2002, **41**, 1925-1928.
5 K. Kim, O. G. Tsay, D. A. Atwood and D. G. Churchill, *Chem. Rev.*, 2011, **111**, 5345-5403.
6 R. A. Sheldon, I. Arends and U. Hanefeld, *Green Chemistry and Catalysis*. Wiley-VCH, Weinheim, 2007.
7 C. C. Romao, F. E. Kuhn and W. A. Herrmann, *Chem. Rev.*, 1997, **97**, 3197-3246.
8 S.-S. Wang and G.-Y. Yang, *Chem. Rev.*, 2015, **115**, 4893-4962.
9 I. V. Kozhevnikov, *Chem. Rev.*, 1998, **98**, 171-198.
10 C. L. Hill and C. M. Prossermccartha, *Coord. Chem. Rev.*, 1995, **143**, 407-455.
11 S. R. Livingston and C. C. Landry, *J. Am. Chem. Soc.*, 2008, **130**, 13214-13215.
12 S. R. Livingston, D. Kumar and C. C. Landry, *J. Mol. Cat. A. Chem.*, 2008, **283**, 52-59.

13 C. R. Ringenbach, S. R. Livingston, D. Kumar and C. C. Landry, *Chem. Mater.*, 2005, **17**, 5580-5586.
14 B. Zhang, S. Li, A. Pothig, M. Cokoja, S. L. Zang, W. A. Herrmann and F. E. Kuhn, *Z. Naturforsch. B*, 2013, **68**, 587-597.
15 C. T. Buru, P. Li, B. L. Mehdi, A. Dohnalkoya, A. E. Platero-Prats, N. D. Browning, K. W. Chapman, J. T. Hupp and O. K. Farha, *Chem. Mater.*, 2017, **29**, 5174-5181.
16 K. E. Cantwell, P. E. Fanwick and M. M. Abu-Omar, *ACS Omega*, 2017, **2**, 1778-1785.
17 T. D. Phan, M. A. Kinch, J. E. Barker and T. Ren, *Tetrahedron Lett.*, 2005, **46**, 397-400.
18 D. Thompson, Y. Zhang and T. Ren, *J. Mol. Cat. A: Chem.*, 2014, **392**, 188-193.
19 D. J. Thompson, Z. Cao, E. C. Judkins, P. E. Fanwick and T. Ren, *Inorg. Chim. Acta*, 2015, **437**, 103-109.
20 F. A. Cotton and G. Wilkinson, *Advanced Inorganic Chemistry*. Wiley, 1988.
21 B. M. Trost and Y. Masuyama, *Isr. J. Chem.*, 1984, **24**, 134-143.
22 H. Y. Lu, C. L. Deng, W. Z. Ren and X. Yang, *Fuel Proc. Technol.*, 2014, **119**, 87-91.
23 G. Absillis, E. Cartuyvels, R. Van Deun and T. N. Parac-Vogt, *J. Am. Chem. Soc.*, 2008, **130**, 17400-17408.
24 B. M. Trost and Y. Masuyama, *Tetrahedron Lett.*, 1984, **25**, 173-176.
25 V. S. Sergienko, *Crystallography Rep.*, 2008, **53**, 18-46.
26 M. C. Carreno, *Chem. Rev.*, 1995, **95**, 1717-1760.
27 Y.-C. Yang, *Acc. Chem. Res.*, 1998, **32**, 109-115.
28 K. Kamata, T. Hirano, R. Ishimoto and N. Mizuno, *Dalton Trans.*, 2010, **39**, 5509-5518.
29 M. Wilm and M. Mann, *Anal. Chem.*, 1996, **68**, 1-8.
30 P. Chen, *Angew. Chem. Int. Ed.*, 2003, **42**, 2832-2847.
31 D. K. Walanda, R. C. Burns, G. A. Lawrance and E. I. von Nagy-Felsobuki, *J. Chem. Soc., Dalton Trans.*, 1999, 311-321.
32 H. Mimoun, I. S. Deroch and L. Sajus, *Bull. Soc. Chim. Fr.*, 1969, 1481.
33 J. M. Bregeault, M. Vennat, L. Salles, J. Y. Piquemal, Y. Mahha, E. Briot, P. C. Bakala, A. Atlamsani and R. Thouvenot, *J. Mol. Cat. A. Chem.*, 2006, **250**, 177-189.
34 C. J. Carrasco, F. Montilla, E. Alvarez, C. Mealli, G. Manca and A. Galindo, *Dalton Trans.*, 2014, **43**, 13711-13730.
35 R. A. J. O'Hair, *Chem. Commun.*, 2006, 1469-1481.
36 R. A. J. O'Hair and G. N. Khairallah, *J. Cluster Sci.*, 2004, **15**, 331-363.

Table of Content Entry

$[Mo_2O_{11}]^{2-}$ identified as the active species in H_2O_2 oxygenation of sulfides catalyzed by heptamolybdate using *in situ* nano-ESI MS analysis